AD-A087 442 DAVID W TAYLOR NAVAL SHIP RESEARCH AND DEVELOPMENT CE--ETC F/G 11/6
DETERMINATION OF FATIGUE DAMAGE.(U)
AUG 80 R N PANGBORN, T TSAKALAKOS, W E MAYO
UNCLASSIFIED DTNSRDC-80/093 NL

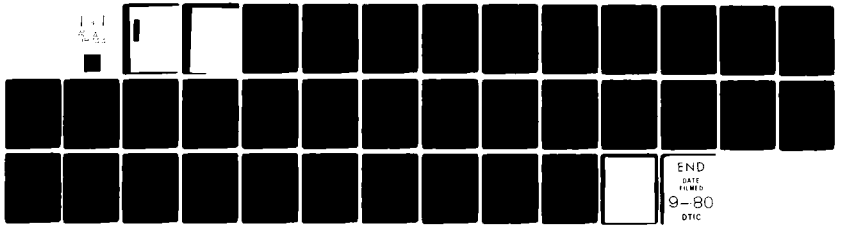

END
DATE FILMED
9-80
DTIC

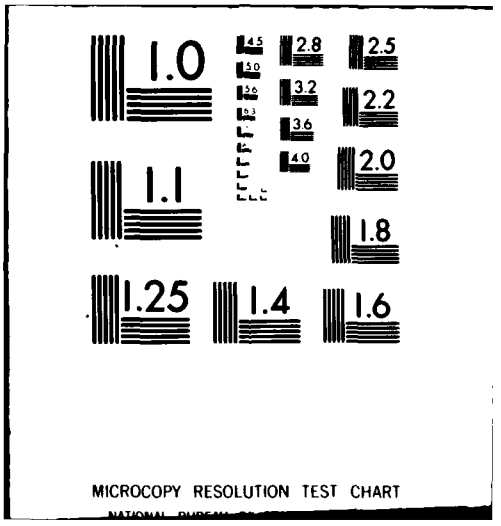
1.0
1.1
1.25
1.4
1.6
1.8
2.0
2.2
2.5
2.8
3.2
3.6
4.0
4.5
5.0
5.6
6.3
MICROCOPY RESOLUTION TEST CHART

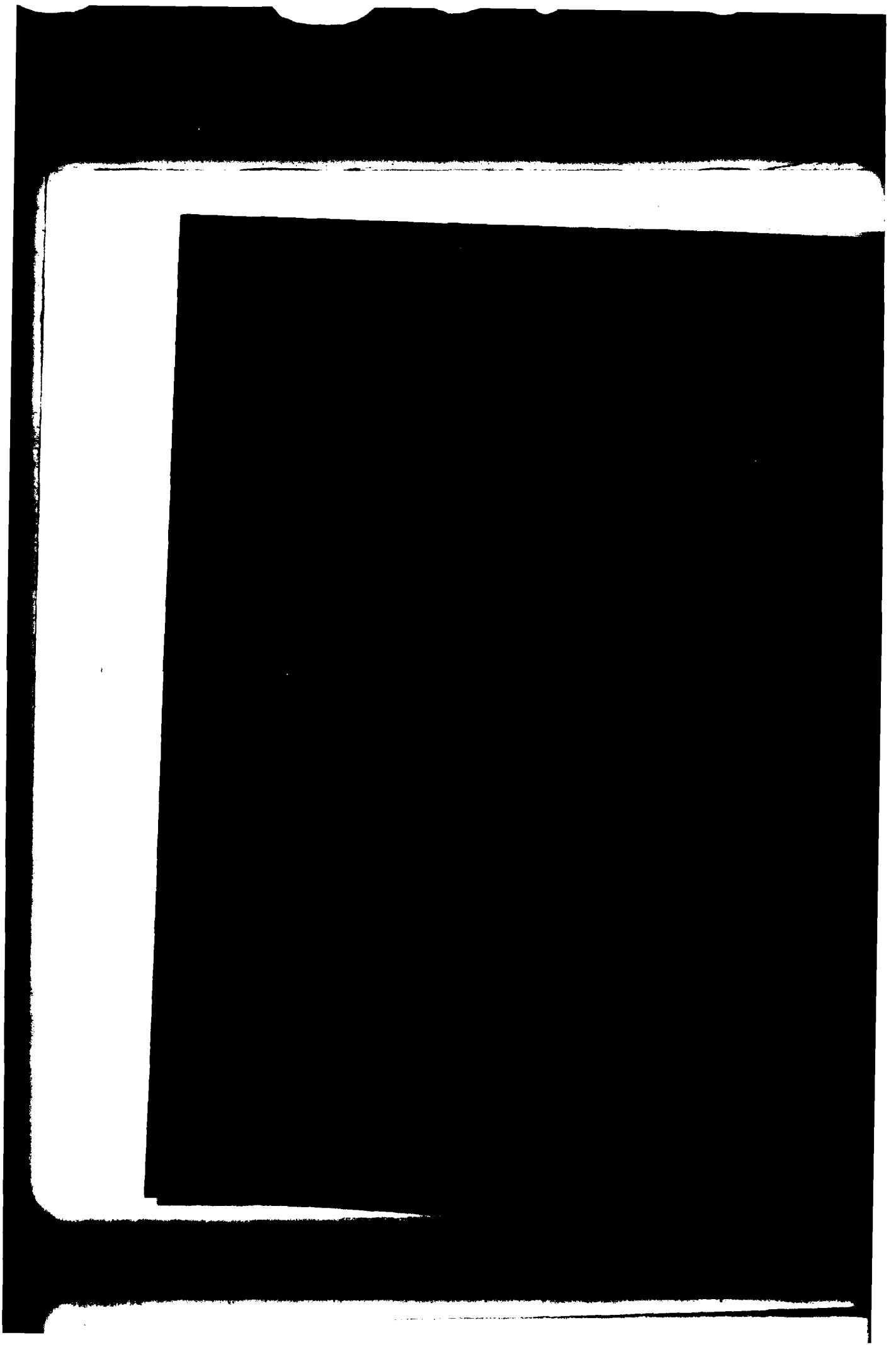

UNCLASSIFIED

SECURITY CLASSIFICATION OF THIS PAGE (When Data Entered)

REPORT DOCUMENTATION PAGE	READ INSTRUCTIONS BEFORE COMPLETING FORM
1. REPORT NUMBER: DTNSRDC-80/093 ✓	2. GOVT ACCESSION NO.: AD-A087442
3. RECIPIENT'S CATALOG NUMBER:	
4. TITLE (and Subtitle): DETERMINATION OF FATIGUE DAMAGE	5. TYPE OF REPORT & PERIOD COVERED: Research and Development Interim Report
	6. PERFORMING ORG. REPORT NUMBER:
7. AUTHOR(s): (See reverse side)	8. CONTRACT OR GRANT NUMBER(s):
9. PERFORMING ORGANIZATION NAME AND ADDRESS: David W. Taylor Naval Ship R&D Center, Bethesda, Maryland 20084	10. PROGRAM ELEMENT, PROJECT, TASK AREA & WORK UNIT NUMBERS: Program Element 61152N; Task Area ZR 022-0101; Work Unit 2002-004
11. CONTROLLING OFFICE NAME AND ADDRESS: David W. Taylor Naval Ship R&D Center, Bethesda, Maryland 20084	12. REPORT DATE: August 1980
	13. NUMBER OF PAGES: 35
14. MONITORING AGENCY NAME & ADDRESS(if different from Controlling Office):	15. SECURITY CLASS. (of this report): UNCLASSIFIED
	15a. DECLASSIFICATION/DOWNGRADING SCHEDULE:

16. DISTRIBUTION STATEMENT (of this Report)

APPROVED FOR PUBLIC RELEASE; DISTRIBUTION UNLIMITED

DTIC ELECTE AUG 5 1980 A

17. DISTRIBUTION STATEMENT (of the abstract entered in Block 20, if different from Report)

18. SUPPLEMENTARY NOTES

19. KEY WORDS (Continue on reverse side if necessary and identify by block number)

Fatigue
Aluminum
X-Ray Diffraction

20. ABSTRACT (Continue on reverse side if necessary and identify by block number)

The deformation response of polycrystalline AA2024-T4 to cyclic loading has been determined by conventional and double-crystal diffractometry.

These studies show a preferential work-hardening near the surface compared to the bulk. The defect distribution as a function of depth was also investigated as a function of the fraction of fatigue life. From these studies, it was determined that the remaining fatigue life could be predicted

(Continued on reverse side)

next page

DD FORM 1 JAN 73 1473 EDITION OF 1 NOV 65 IS OBSOLETE S/N 0102-LF-014-6601

UNCLASSIFIED

SECURITY CLASSIFICATION OF THIS PAGE (When Data Entered)

(Block 7)

R. N. Pangborn (Pennsylvania State University)
T. Tsakalakos, W. E. Mayo, S. Weissmann (Rutgers University)
I. R. Kramer (David W. Taylor Naval Ship R&D Center)

(Block 20 continued)

by determining the average ratio β/β^* where β is the linewidth at any number of fatigue cycles and β^* is the critical linewidth at fracture. Current studies have shown these predictions to be valid for tests where the stress amplitude is held constant for the entire test. A few tests have also been performed where the loading sequence is more complicated. In these tests, the X-ray predictive method was found to be far more accurate than conventional methods.

TABLE OF CONTENTS

LIST OF FIGURES

Page

TABLE

ABSTRACT

The deformation response of polycrystalline AA2024-T4 to cyclic loading has been determined by conventional and double-crystal diffractometry.

These studies show a preferential work-hardening near the surface compared to the bulk. The defect distribution as a function of depth was also investigated as a function of the fraction of fatigue life. From these studies, it was determined that the remaining fatigue life could be predicted by determining the average ratio β/β^* where β is the linewidth at any number of fatigue cycles and β^* is the critical linewidth at fracture. Current studies have shown these predictions to be valid for tests where the stress amplitude is held constant for the entire test. A few tests have also been performed where the loading sequence is more complicated. In these tests, the X-ray predictive method was found to be far more accurate than conventional methods.

ADMINISTRATIVE INFORMATION

This investigation is part of an in-house research program at the David W. Taylor Naval Ship Research and Development Center (DTNSRDC). It was conducted under Program Element 61152N, Task Area ZR 022-0101, Work Unit 2082-004.

INTRODUCTION

Early investigations of fatigue failure in metals provided substantial evidence of the surface sensitivity of mechanical behavior. Surface studies revealed the formation of slip bands and their topological development into intrusions and extrusions associated with subsequent crack initiation and eventual failure.[1-4*] Other fatigue investigations focused on the microstructural developments in metals during repeated stressing.[5-9] During the 1960s, many studies were performed to relate the fatigue-induced defect structure with the slip morphology exhibited on the surface.[10-14]

---

*A complete listing of references is given on page 29.

While surface effects were recognized as a controlling factor in fatigue performance, early X-ray methods were incapable of predicting the impending onset of fatigue failure or even the span of the fatigue life.[15,16] Line broadening was observed after cycling over a small fraction of the total fatigue life, but then it remained virtually unaltered both in extent and intensity throughout the remainder of the life.

A recent application of a special X-ray method[17,18] to cyclically stressed 2024 Al enabled the prediction of both the fatigue life and failure of the aluminum with a considerable degree of accuracy. This nondestructive method for analysis of the fatigue-induced defect structure is based on the principle of X-ray double-crystal diffractometry and employs X-ray topography to afford a visualization of the defect configuration. The polycrystalline specimen is irradiated with a crystal-monochromated beam; and each reflecting grain is considered to function independently as the test crystal of a double-crystal diffractometer. Depending on the perfection of the grains, the specimen is rotated in intervals of seconds or minutes of arc; and the spot reflections, recorded along the Debye arcs of a cylindrical film for each discrete specimen rotation, are separated by film shifts. This multiple-exposure technique gives rise to an array of spots for each reflecting grain. These arrays of spots, with their intensity dependent on specimen rotation, represent X-ray rocking curves of the reflecting grains. Thus, if the grains contain a substructure, the intensity distribution of the arrays of diffraction spots will be multipeaked not only along the horizontal, but also along the azimuthal elevation. From the angle subtending successive peaks of the rocking curve, the excess dislocation density between subgrains can be determined; while the excess dislocation density within the subgrain can be obtained from the spread of the subpeak curve. From the width β, at half the maximum intensity, the excess dislocation density of the entire grain is determined.[17,18]

By analyzing various (hkℓ) reflections, a representative statistical parameter $\overline{\beta}$ of the defect structure of the grain population is obtained. Furthermore, by taking Berg-Barrett reflection topographs and performing

a spatial tracing at the reflections to the spot reflections of the rocking curve, the analyzed rocking curve can be correlated to the grain topography on the specimen.[18]

The double-crystal diffractometer arrangement has been successfully employed to study single crystals, pure polycrystalline metals, and multiphase alloys with ease. The method offers good resolution of the local effects in individual grains, but also provides information from a sufficient number of grains to permit accurate statistical analysis of an average or mean microstructural response. The film-recorded reflections represent an imaging of the subdomain structure which can also be interpreted quantitatively in terms of the excess dislocation density, which is known to be a factor in the accumulation of fatigue damage and the ultimate initiation of fracture. The purpose of the present study is to exploit these aspects of the X-ray method to isolate a suitable microstructural indicator of progressive fatigue damage, and thereby contribute to the capability for accurate determination of the fatigue life and failure prediction. In accomplishing this objective, the double-crystal diffractometer is particularly useful for the microstructural analysis of both the surface and the bulk. Analysis of these regions can be carried out independently, in a stepwise manner, by incremental removal of surface layers. In addition, nondestructive in-depth analysis is made possible by altering the depth of penetration of the incident radiation. This potential may be very important in technological applications when service components are to be examined.

A method which can be used in conjunction with the double-crystal technique described above is the Warren-Averbach (WA) method of Fourier analysis of X-ray line broadening. This technique is unique in that the sizes of coherently reflecting domains and the internal microstrains can be determined simultaneously. Alternate theories of line broadening assume that broadening of Bragg peaks is due predominately to either size or strain, but not both. The WA method is unique in that multiple sources of line broadening may be operating simultaneously.

Two peaks are selected for the WA analysis, usually the 200 and 400 Bragg reflections. A counter is used to record the intensity distribution, and the intensity peaks at 0.005-degree increments are fed into a PDP 11-34 computer. The Rachinger graphical separation of the $K\alpha_1$ and $K\alpha_2$ double profile is employed (see Appendix A); and the $K\alpha_1$ corrected profile of both annealed and worked samples is used in the analysis. The Stokes method is used for the correction of the instrumental broadening.

A FORTRAN computer program was written (see Appendix B) for calculating the Stokes-corrected Fourier coefficients of a broadened profile. According to the WA analysis, the corrected Fourier coefficients are related to the particle size and the root-mean-square microstrains as follows:

$$\ln A_L(h_0) = \ln A_L^S - \frac{2\pi^2 L^2}{a^2} < \varepsilon_L^2 > h_0^2 \qquad (1)$$

where A_L = the corrected Fourier coefficients

A_L^S = the corrected Fourier coefficients of particle size

L = the distance normal to the reflecting planes

$h_0^2 = h^2 + k^2 + \ell^2$

a = the lattice parameter

By plotting $\ln A_L(h_0)$ versus h_0^2 (usually for two reflections) the size effect and microstrains can be separated. The intercepts of these plots provide the particle size coefficients A_L^S for various L and from the slopes the microstrains can be calculated.

PREVIOUS WORK

Several reports covering previous work under this program have been published recently.[19-21] These elucidate the preferential work hardening occurring at the surface of fatigued AA2024-T4 samples and the associated excess dislocation densities for grains near the surface. It was found

that an initial rapid increase in $\overline{\beta}$ comprised the first 20 to 25 percent of the life followed by a long intermediate period featuring very little structural change and a final rapid enhancement during the last 5 to 10 percent of the life, coinciding with crack initiation and growth. It was found that a critical excess dislocation density exists which is associated with fatigue fracture. This critical value was independent of the stress amplitude and varied according to a Petch-type relationship for different grain sizes of the same alloy. An in-depth analysis, carried out by stepwise removal of the surface layers of cycled specimens, disclosed a plastic response for the grains located in the bulk after about 5 percent of the fatigue life. The defect structure in the specimen core developed gradually during the cycling. The excess dislocation density for the bulk increased almost linearly as a function of the fatigue life, with a terminal value at failure identical to the critical excess dislocation density for surface grains. The fatigue process was interpreted as a rapid work hardening of the surface to form a barrier to dislocation egression and rearrangement. The dynamic interplay between the surface barrier and the eventual plastic response activated in the bulk leads to a critical defect accumulation at the surface and incipient cracking.

When the fatigue process was interrupted prior to failure and the surface layer was removed, a striking recovery phenomenon was observed throughout the specimen cross section during subsequent cycling. The bulk defect structure was thus shown to be extremely unstable in the absence of the restraining influence imposed by the work-hardened surface layer. The extension of the fatigue life of metals by judicious surface removal was ascribed primarily to the elimination of the surface barrier, rather than to the removal of microcracks.

The fatigue response at various depths from the surface was also investigated nondestructively by employing X-ray radiation with differing penetration capabilities. The excess dislocation density of grains located up to 300 micrometers in depth was examined using molybdenum radiation and was found to vary linearly with the fatigue life. This steep, linear dependence, in conjunction with the early life saturation

behavior of surface-grain densities measured with copper radiation, provided a new criterion for predicting accurately the fatigue life and failure.

PRESENT WORK

The striking feature of the previous work is that a linear relationship exists between the statistical average $\overline{\beta}$ and the remaining fatigue life. This enabled accurate prediction of the useful remaining life by a simple nondestructive determination of $\overline{\beta}$ using Mo radiation. However, these results were strictly applicable only to samples tested at a constant stress amplitude. Although tests indicated that $\overline{\beta}^*$ was stress amplitude independent, it was not clear how a single sample would behave under more complex loading histories. Accordingly, the present tests were undertaken to determine the applicability of the X-ray double-crystal diffractometry technique for predicting fatigue failure in samples with a random stress loading sequence.

The spectral loading sequence chosen is shown in Figure 1. Four stress levels were selected between 25 ksi and 41 ksi, corresponding approximately to the fatigue limit and the proportional limit, respectively. The number of cycles at each stress level was determined by setting each loading step to 20 percent of the fatigue life at each stress level. The stress versus number of cycles (S-N) curve for such a determination is shown in Figure 2 and was obtained for a constant stress amplitude ($R = -1$).

After each loading step, the sample was analyzed using the double-crystal diffractometer with Mo radiation to determine the rocking curve halfwidth. The value of $\overline{\beta}$ obtained after each step was then compared to the calibration curve shown in Figure 3. This curve was determined in the previous studies on constant amplitude fatigue cycling. At the end of the fourth loading cycle (41 ksi), $\overline{\beta}$ was determined and located on the calibration curve. As shown in Figure 4, the predicted remaining life was 39 percent based on the X-ray method. Figure 4 also shows the predicted remaining fatigue life of 20 percent based on the conventional technique using the S-N curve. The actual remaining fatigue life was

found to be 42.5 percent. Therefore, the error in estimating the remaining life on the basis of the usual techniques was over 100 percent; while the error of the X-ray technique was less than 10 percent.

Analyses using line broadening techniques and conventional diffractometry have also been performed. After each stage of cycling, a conventional diffractometer trace is run to determine the peak halfwidths for the 111, 200, 222, and 400 peaks; and corrections are made to take into account variations in the initial halfwidths. If a Cauchy line profile is assumed, it can be shown[22] that the line broadening is related to the coherently reflecting domain size ℓ and the strain e through the equation

$$dS_0 = \frac{1}{\ell} + 2eS \tag{2}$$

where $S = 2\sin\theta/\lambda$

$dS = 2\cos\theta d\theta/\lambda$

θ = Bragg angle for hkℓ reflection

λ = X-ray wavelength

The quantity $2d\theta$ is equivalent to $\overline{\beta}$, the peak halfwidth; and, by a simple substitution, Equation (2) becomes

$$\overline{\beta}\cos\theta = \frac{\lambda}{\ell} + 4e\sin\theta \tag{3}$$

By a linear regression analysis, the quantities ℓ and e can be readily determined from the experimentally measured $\overline{\beta}$. As shown in Figure 5, the relationship between $\overline{\beta}\cos\theta$ and $\sin\theta$ is indeed linear for the four fractions of life investigated (N/N_F = 0.22, 0.28, 0.42, and 0.57). The slope of each line is equal to 4e and the intercept is λ/ℓ.

Once the values of e and ℓ are determined, the individual contributions to the dislocation density ρ_e and ρ_ℓ can be determined through the equations

$$\rho_e = \frac{12}{b^2} < \varepsilon^2 > = \frac{7.68}{b^2} e^2 \qquad (4a)$$

$$\rho_\ell = \frac{1}{\ell^2} \qquad (4b)$$

$$\overline{\rho} = (\rho_e \rho_\ell)^{1/2} \qquad (4c)$$

The quantities ρ_e, ρ_ℓ, and $\overline{\rho}$ derived from Figure 5 are summarized in Table 1 along with the quantities e and ℓ. Note that the coherently diffracting domain size remains nearly constant over the life interval 0.22 to 0.57, while the strain steadily increases.

TABLE 1 - LINE BROADENING ANALYSIS BY CONVENTIONAL DIFFRACTOMETER

Fraction of Life $-(N/N_F)$	Strain $-e$	Domain Size (Å) $-\ell$	Dislocation Density (cm^{-2}) ρ_e	Dislocation Density (cm^{-2}) ρ_ℓ	Root Mean Dislocation (cm^{-2}) $(\rho_e \rho_\ell)^{1/2}$
0.22	0.00157	319	2.33×10^{10}	9.83×10^{10}	4.79×10^{10}
0.28	0.00322	462	9.77×10^{10}	4.69×10^{10}	6.77×10^{10}
0.42	0.00406	344	15.50×10^{10}	8.45×10^{10}	11.44×10^{10}
0.57	0.00436	305	17.86×10^{10}	10.80×10^{10}	13.89×10^{10}

Both quantities ρ_e and $\bar{\rho}$ are linearly related to the fraction of life N/N_F, as shown in Figures 6 and 7. The best fit is obtained by utilizing $\bar{\rho}$, which includes variations in both ρ_e and ρ_ℓ. The error between the experimental value of $\bar{\rho}$ and the value obtained from the linear regression is in no case worse than 10 percent. Thus, these types of measurements should be capable of being used to accurately predict the remaining life. Subsequent experiments are being initiated to verify this assumption.

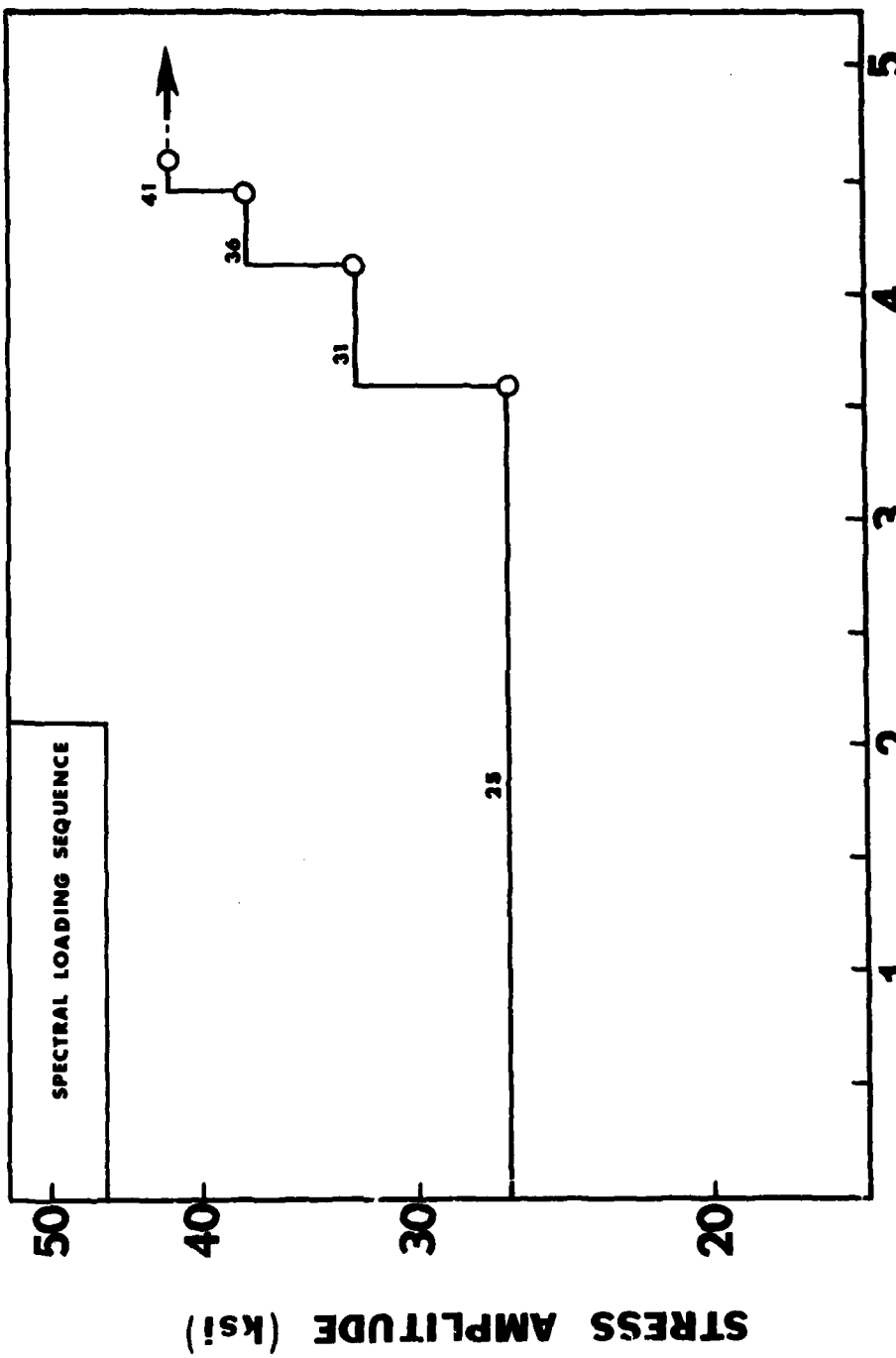

Figure 1 - Spectral Loading Sequence for AA2024-T4 Samples

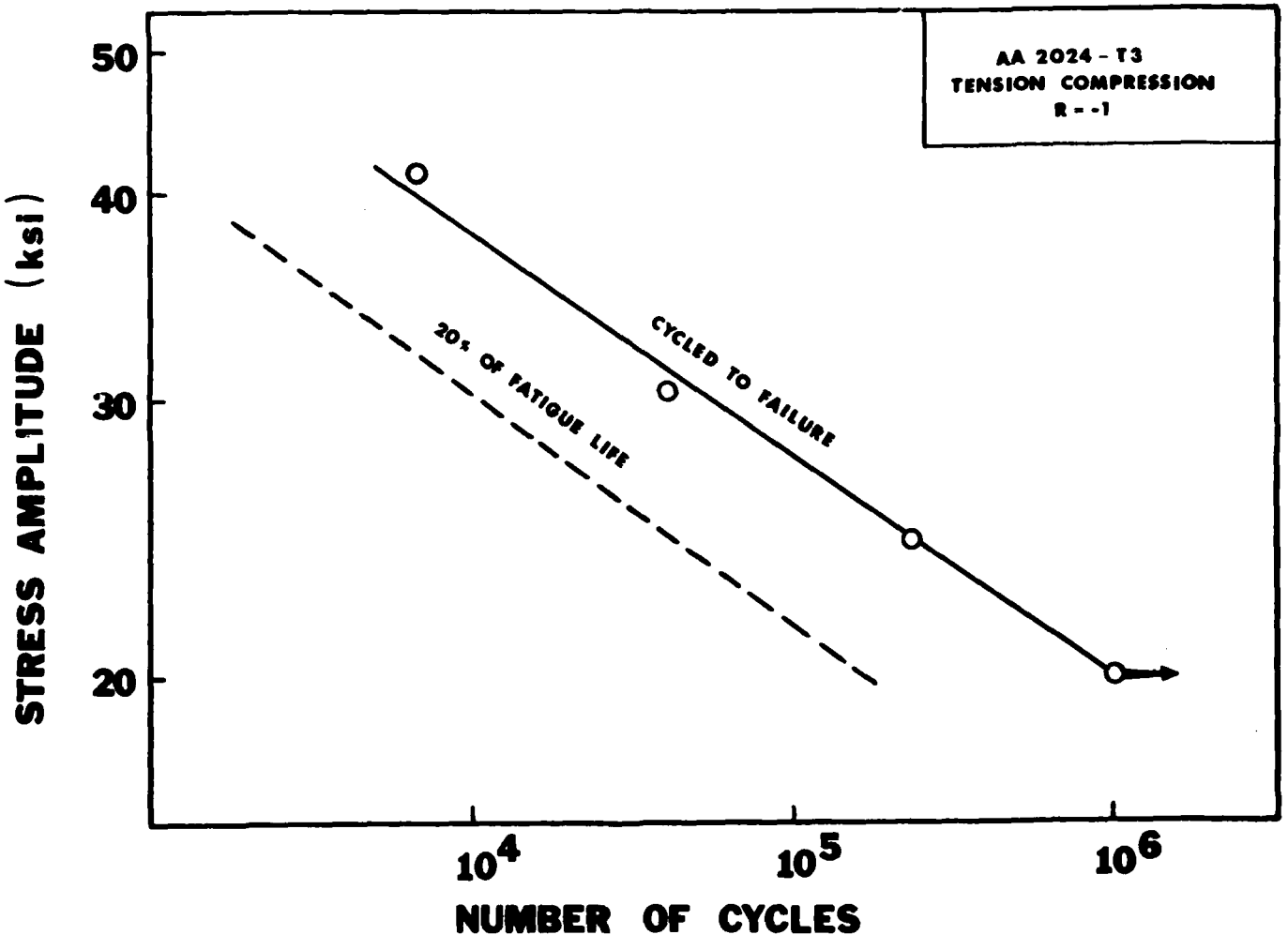

Figure 2 - Fatigue Curve Determined from Constant Stress Amplitude Tests

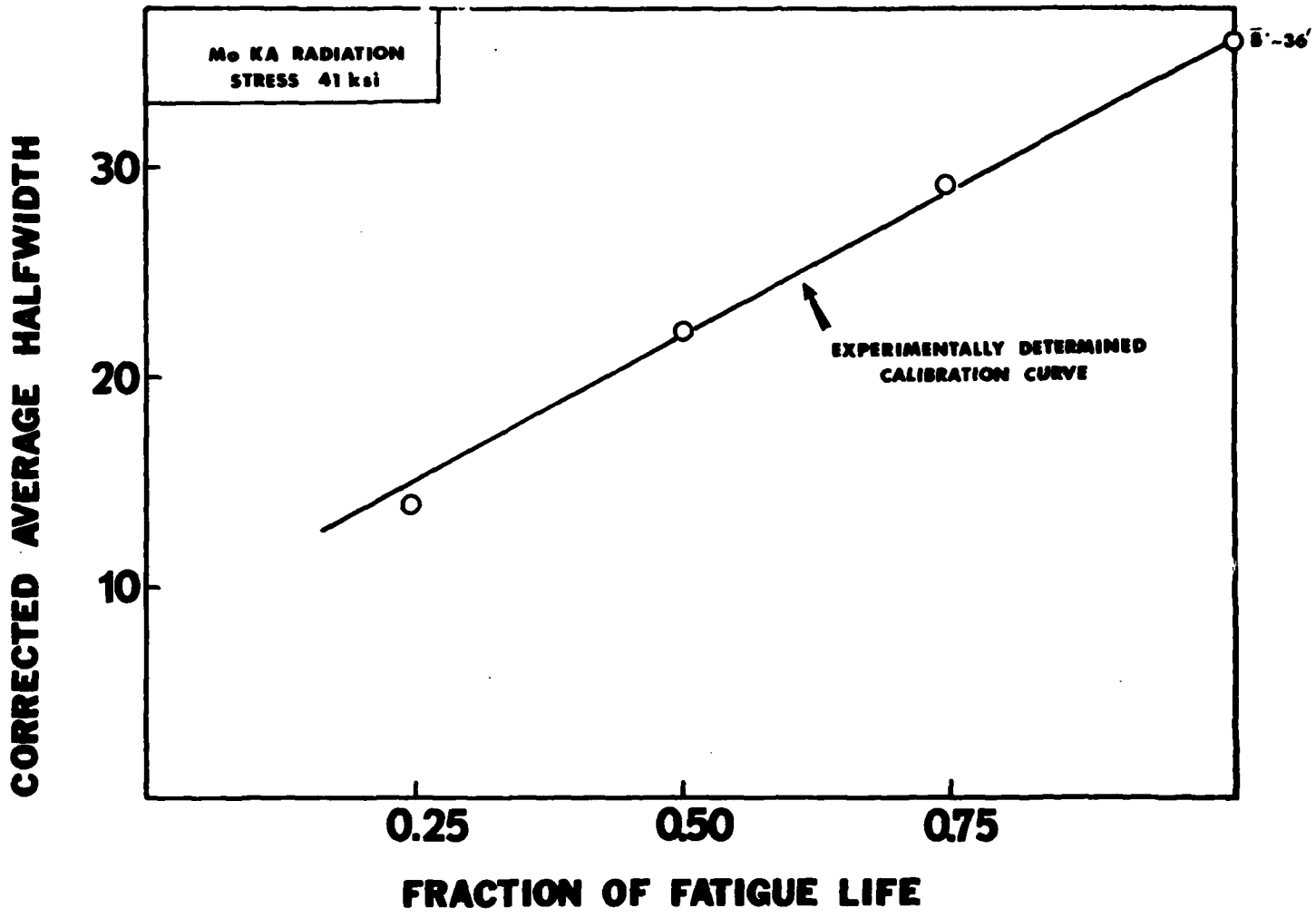

Figure 3 - Experimentally Determined Calibration Curve of Corrected Average Halfwidth as a Function of Fatigue Life

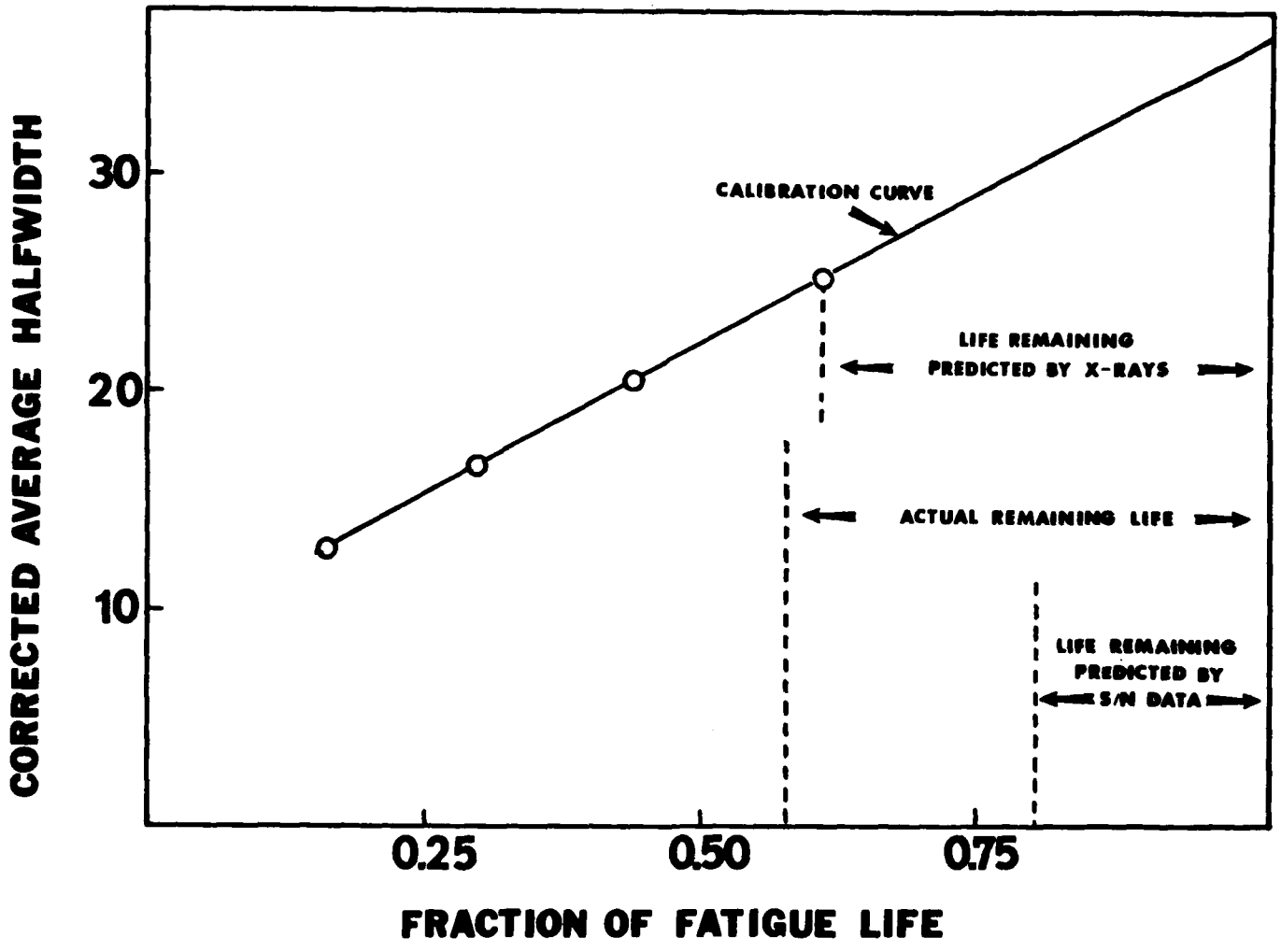

Figure 4 - Results of Spectral Loading Experiment Comparing Predicted Remaining Fatigue Life and Actual Remaining Life

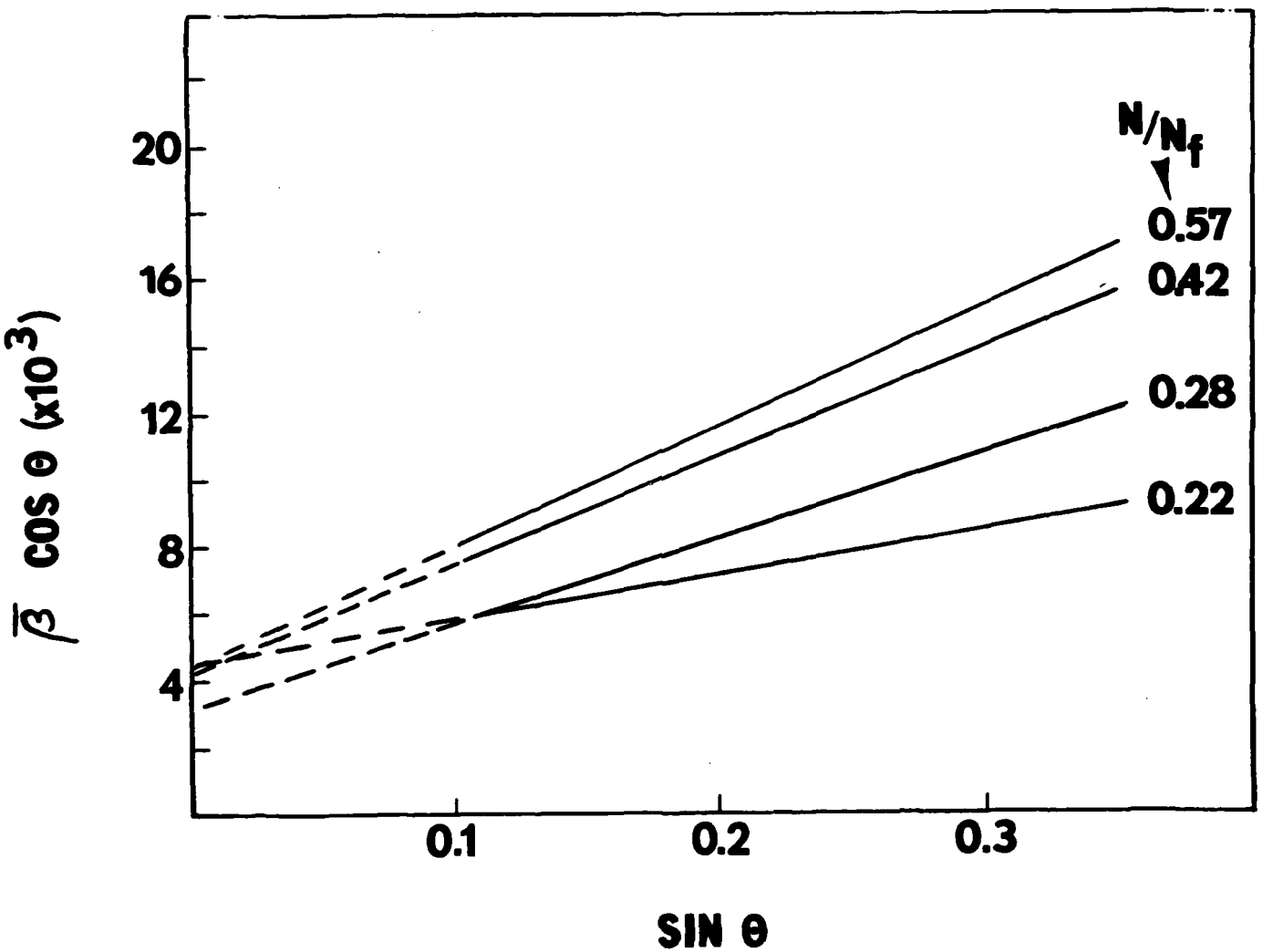

Figure 5 - Results of Conventional Diffractometer Study for Various Fractions of Fatigue Life, N/N_F

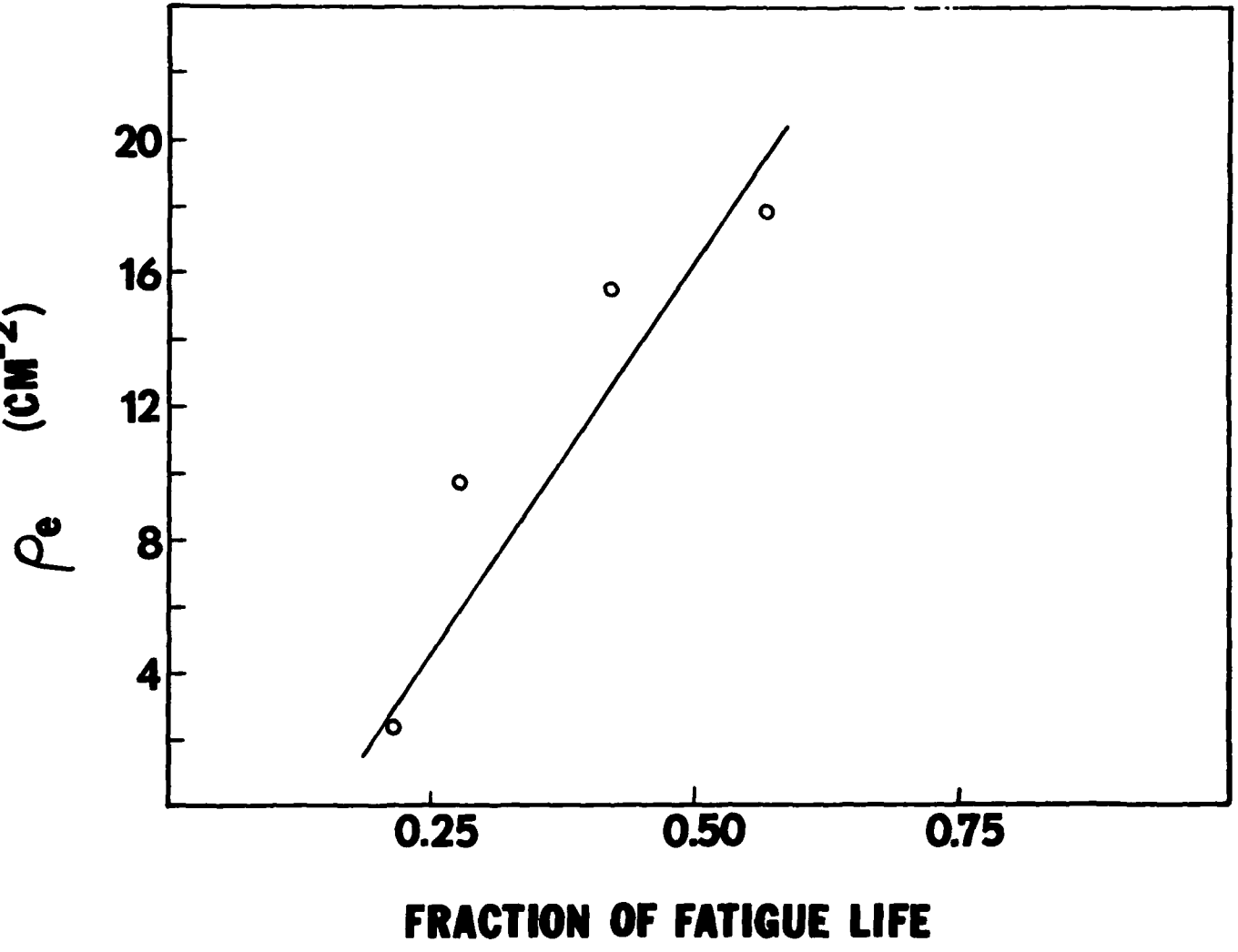

Figure 6 - Correlation Between Strain Dislocation Density ρ_e and Fraction of Fatigue Life

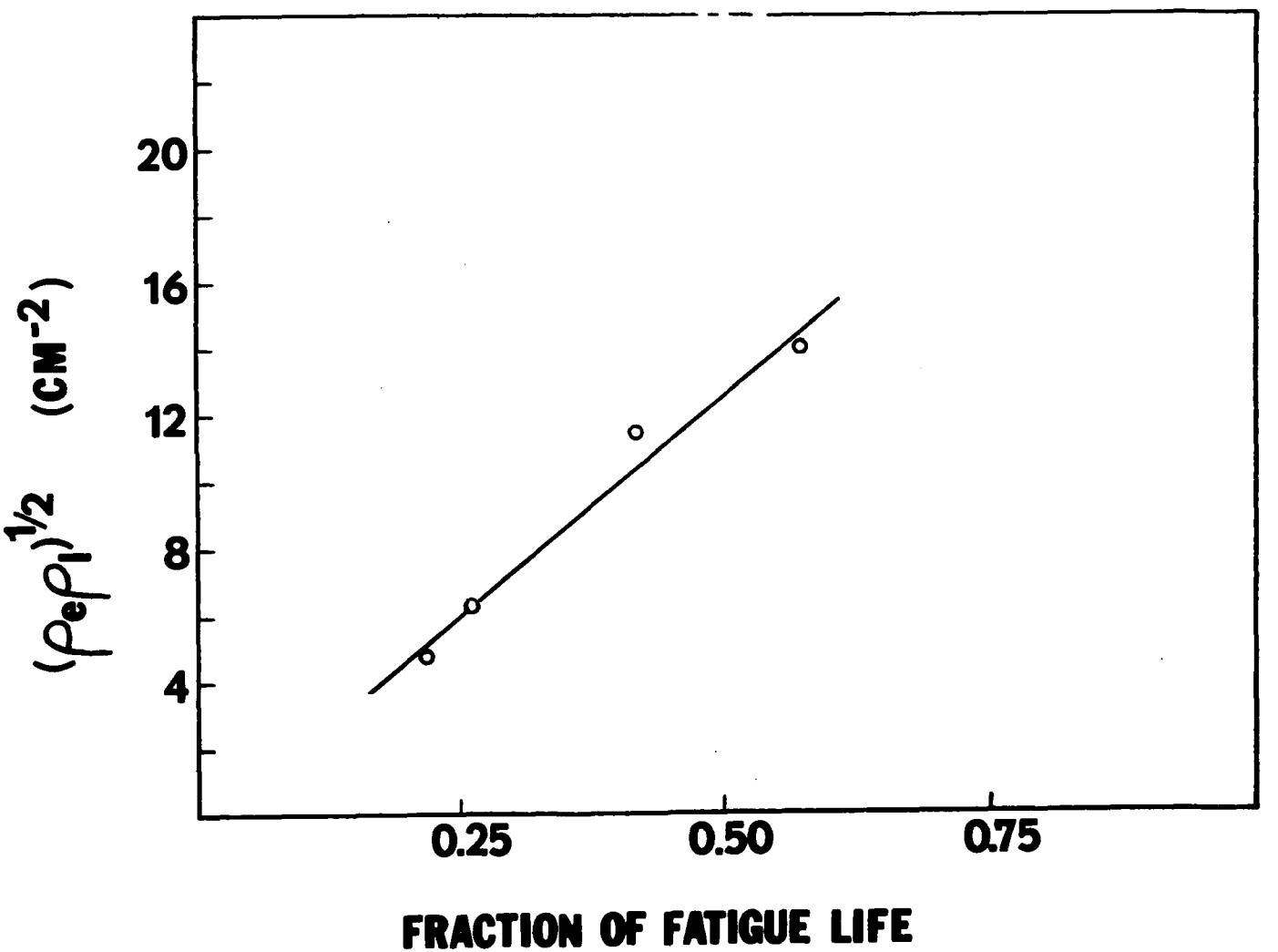

Figure 7 - Correlation Between Mean Dislocation Density and Fraction of Fatigue Life

APPENDIX A

FORTRAN PROGRAM FOR RACHINGER SEPARATION OF $K\alpha_1$ AND $K\alpha_2$ PEAKS

```
C       THERE EXISTS DIFFERENCES BETWEEN THE
C       UPDATED HARD COPY AND THIS VERSION OF THE PROGRAM
C
        PROGRAM  RACHC
        IMPLICIT INTEGER (A-Z)
        INTEGER  TLU,NP,IDEL2
        REAL     CPS(500),DEL,IDEL,YINC,SUM,A,B,C,FRA
        REAL*8 FSPEC
        REAL*4 DEV
        LOGICAL*1 DSN(10),TEM(3)
        DATA DEV/3RDX1/
        DO 40I=1,10
40      DSN(I)=' '
        GO TO 16
15      WRITE(5,20)
        DO 43I=1,10
43      DSN(I)=' '
20      FORMAT(/' FILENAME MUST BE 6 CHARACTERS WITH 3 CHARACTER
     * EXTENSION.',/,'      EX:  'FILNAM.DAT' (OMIT QUOTES)',///,' RE-')
16      WRITE (5,1)
1       FORMAT(' ENTER THE FILE NAME:',$)
        READ(5,2)(DSN(I),I=1,10)
2       FORMAT(10A1)
        I=1
3       IF (DSN(I).EQ.'.') GO TO 12
        I=I+1
        IF (I.EQ.10) GO TO 11
        GO TO 3
12      IF (I.GT.7) GO TO 15
        TEM(1)=DSN(I+1)
        TEM(2)=DSN(I+2)
        TEM(3)=DSN(I+3)
        DSN(7)=TEM(1)
        DSN(8)=TEM(2)
        DSN(9)=TEM(3)
        IF (I.EQ.7) GO TO 11
        DO 99K=I,6
99      DSN(K)=' '
11      DSN(10)=' '
        J = IRAD50(9,DSN,FSPEC)
        I = IASIGN(9,DEV,FSPEC)
        TLU=5
17      FORMAT(/,' ENTER THE 2 THETA SEPERATION BETWEEN THE
     *ALPHA 1 AND 2:',$)
37      FORMAT(/,' ENTER THE RATIO BETWEEN THE ALPHA 1 AND ALPHA 2:',$)
41      FORMAT(/,' INTEGRATED AREA CORRECTED FOR ALPHA 1, ALPHA 2 =',F9.2)
        READ(9,97)NP
97      FORMAT(I3)
        DO30I=1,NP
        READ(9,96)CPS(I)
96      FORMAT(F12.6)
30      CONTINUE
        A=0.
        B=0.
        DO42I=1,10
        A=A+CPS(I)/10.
42      B=B+CPS(NP+1-I)/10.
        DO38I=1,NP
38      CPS(I)=CPS(I)-(A+(B-A)*(I-1)/(NP-1.))
        WRITE(TLU,17)
        READ(TLU,6)DEL
6       FORMAT(F12.6)
        WRITE(5,7)
7       FORMAT(/,' ENTER YINC:',$)
        READ(5,8)YINC
```

```
8       FORMAT(F12.6)
        IDEL=DEL/YINC
        DEL=DEL/YINC
        C=DEL-IDEL
        SUM=0.0
        IDEL2=INT(IDEL)
        DO100I=1,IDEL2
100     SUM=SUM+CPS(I)
        WRITE(TLU,37)
        READ(TLU,9)FRA
9       FORMAT(F12.6)
        DO110I=IDEL+1,NP
        CPS(I)=CPS(I)-(CPS(I-IDEL+1)-(CPS(I-IDEL+1)-CPS(I-IDEL))*C)*FRA
110     SUM=SUM+CPS(I)
        WRITE(5,98)
98      FORMAT(/,' THE PRINTED DATA SET WILL BE ALLOWED TO BE STORED ON',
     $/,' DISC AFTER THE RESULTS HAVE BEEN VERIFIED.')
        DO350I=1,NP
        WRITE(6,95)CPS(I)
350     CONTINUE
95      FORMAT(F12.6)
        WRITE(TLU,41)SUM
        END
```

APPENDIX B

FORTRAN PROGRAM FOR CALCULATING THE STOKES-CORRECTED FOURIER COEFFICIENTS

```
      REAL*4 DEV
      REAL*4 DEV2
      REAL*4 FILE(2)
      REAL*4 FILE2(2)
      DATA DEV/3RDX1/
      DATA DEV2/3RDX1/
      DATA FILE/6RWORKED,3RDAT/
      DATA FILE2/6RANEALD,3RDAT/
      I=IASIGN(9,DEV,FILE)
      I=IASIGN(8,DEV2,FILE2)
      DEFINE FILE 9(500,4,U,NREC)
      DEFINE FILE 8(500,4,U,NREC2)
      REAL XINTA(500),FRA(60),FIA(60)
      REAL XINTW(500),FRW(60),FIW(60)
      REAL FCCR(60),FCCI(60),LNFCR(60)
      REAL SAVE(60)
      REAL LACA,LACW,KV,MA
      INTEGER*4 FLAGS(60)
      INTEGER*4 YES,NO,IANS
      INTEGER TLU,IPRAM(5),TOF,R1W(128),R1A(128),TLEW(32),
     $TLEA(32),DSW,DSA,PPDATA(3),HKL,RADA,RADW,DATE(4),
     $DATEA(4),DS,PAGE,HKLW(4),HL(4)
      REAL*8 DATEW,TIME
      EQUIVALENCE (R1A(1),DSA),(R1A(2),TLEA),(R1A(34),HL),
     $(R1A(40),RADA),(R1A(48),TA),(R1A(50),LACA),(R1A(52),
     $YAINC),(R1A(54),TTHA1),(R1A(56),NPA),(R1A(62),DATEA),(R1A(66),
     $WAVE)
      EQUIVALENCE (R1W(1),DSW),(R1W(2),TLEW),(R1W(34),
     $HKLW),(R1W(40),RADW),(R1W(42),MA),(R1W(44),KV),
     $(R1W(48),TW),(R1W(50),LACW),(R1W(52),YINCW),(R1W(54),TTHW1)
     $,(R1W(56),NPW),(R1W(62),DATEW),(R1W(66),WWAVE)
      DATA YES/3HYES/
      DATA NO/3HNO /
      DATA PPDATA/2HPP,2HDA,2HTA/
      KV=0.0
      DO 6668I=1,60
6668  FLAGS(I)=' '
   1  FORMAT(' THE FOLLOWING REQUESTS ARE FOR THE ANNEALED SAMPLE.')
   2  FORMAT(' WHAT IS THE WAVELENGTH USED')
   5  FORMAT(' ENTER THE MAXIMUM AND MINIMUM TWO THETA VALUES'
     $//' MAX=_',$)
   6  FORMAT(' MIN=_',$)
   9  FORMAT(' R.C.F.C.=REAL CORRECTED FOURIER COEF.',/,
     $     ' I.C.F.C.=IMAGINARY CORRECTED FOURIER COEF.',/,
     $      ' L.F.C.C.=LOG OF THE REAL CORRECTED FOURIER COEF.',/,
     $      ' DISP.   =DISPLACEMENT BETWEEN SAMPLED CELLS',/,
     $      ' R.U.F.C.=REAL UNCORRECTED FOURIER COEF.',/,
     $      ' I.U.F.C.=IMAGINARY UNCORRECTED FOURIER COEF.',/,
     $      ' R.F.C.A.=REAL FOURIER COEF. OF ANNEALED SAMPLE',/,
     $      ' I.F.C.A.=IMAGINARY FOURIER COEF. OF ANNEALED SAMPLE',/,
     $     ' L.U.F.C.R.=LOG OF UN-NORMALIZED REAL FOURIER COEF.',///)
  10  FORMAT(' HARMONIC  R.C.F.C.   I.C.F.C.   L.F.C.C.      DISP.
     $   R.U.F.C.     I.U.F.C.     R.F.C.A.   I.F.C.A.   L.U.F.C.R.')
  16  FORMAT(2X,F5.2,2X,F8.3,2X,F8.3,6X,F6.3,6X,F7.2,2X,F8.3,
     $5X,F8.3,5X,F8.3,3X,F8.3,3X,F8.3,3X,A1)
  18  FORMAT(1X)
  19  FORMAT(' ENTER THE MINIMUM TWO THETA VALUE WHICH WILL EVER BE
     $ ',/,' USED FOR THE BROADEST PEAK USING THIS RADIATION')
  20  FORMAT(' ENTER THE BRAGG ANGLE FOR THE PEAK')
  21  FORMAT(' AAA=',F12.7)
  31  FORMAT(' DO YOU WISH TO ENTER DATA FOR ANOTHER WORKED PEAK
     $ OF THIS REFLECTION?')
  32  FORMAT(A3)
  33  FORMAT(' THE FOLLOWING DATA REQUESTS ARE FOR THE WORKED SAMPLE')
  34  FORMAT(' DO YOU WISH TO CHANGE THE HARMONIC FACTOR FROM 5?')
```

```
  38    FORMAT(' HARMONIC FACTOR= ')
  40    FORMAT(' ENTER THE SAMPLES IDENTIFICATION')
  41    FORMAT(32A2)
  47    FORMAT(//,' PAGE ',I3,/,32A2,/,' DATA WAS TAKEN ',A9,5X,A5)
  48    FORMAT(35X,' INITIAL ',11X,' THICKNESS',/,15X,' RADIATION',11X,
     #'2 THETA',13X,'IN   CM.',/,19X,A2,15X,F6.2,14X,F8.5,//,15X,
     #' MILLIAMPS',11X,'INCREMENT',11X,'ABS. COEF.',/,19X,F4.1,17X,
     #F4.2,12X,F7.2,//,15X,'    KV   ',12X,'POINTS',/,18X,F4.1,15X
     #,I3,//,15X,' MONOCHROMETER',7X,'AAA',17X,'HARMONIC',/,15X,
     #' BRAGG ANGLE',30X,'FACTOR',/,18X,F6.2,8X,F12.6,14X,F6.3,//)
  49    FORMAT(' IS THERE ANOTHER ANNEALED PEAK YOU WISH TO USE
     # FOR A STANDARD ?')
  59    LACA=0.
        TA=0.
        PAGE=1
        WRITE(5,3)
3       FORMAT(' ENTER THE DATE:',$)
        READ(5,4)DATEW
4       FORMAT(A9)
        WRITE(5,7)
7       FORMAT(' ENTER THE TIME:',$)
        READ(5,8)TIME
8       FORMAT(A5)
        WRITE(5,19)
        READ(5,1111)TTLOW
1111    FORMAT(F12.6)
        TLOW=TTLOW*3.1416/360.
        WRITE(5,20)
        READ(5,1111)BRAGG
        BRAGG=BRAGG*3.1416/180
        WRITE(5,1)
86      WRITE(5,40)
        READ (5,41)(TLEA(I),I=1,32)
        WRITE(5,2)
        READ(5,1111)WAVE
        PAUSE 'MOUNT THE DISC CONTAINING THE ANNEALED SAMPLE'
        READ(8'1)NPA
        DO23I=2,NPA+1
        READ(8'I)XINTA(I-1)
23      CONTINUE
24      WRITE(5,5)
        READ(5,1111)TTHA2
        WRITE(5,6)
        READ(5,1111)TTHA1
        YAINC=(TTHA2-TTHA1)/(NPA-1)
350     XMXA=0.00
        DO100I=1,NPA-2
        DINT=XINTA(I)+XINTA(I+1)+XINTA(I+2)
        IF(XMXA.GT.DINT)GOTO100
        XMXA=DINT
        IMXA=I+1
100     CONTINUE
        WRITE(5,3333)WAVE,BRAGG,TLOW
3333    FORMAT(' WAVE=',F12.6,' BRAGG=',F12.6,'TLOW=',F12.6)
        AAA=WAVE/(4.0*(SIN(BRAGG)-SIN(TLOW)))
        WRITE(5,21)AAA
        HF=5.
90      WRITE(5,34)
        READ(5,32)IANS
        IF(IANS.EQ.NO)GOTO92
        IF(IANS.NE.YES)GOTO90
        WRITE(5,38)
        READ(5,1111)HF
92      WRITE (5,451)
451     FORMAT(' WHAT RADIATION WAS USED,
     #(ENTER 2-LETTER CODE FOR TARGET ELEMENT).',/,' ?',$)
```

```
      READ(5,452)RADW
452   FORMAT(A2)
      CALL BKGND(XINTA,NPA)
      CALL LRNTZ(WAVE,TTHA1,NPA,XINTA,YAINC,TLU,TA,LACA,ALPHA)
      CALL FRCOF(IMXA,XINTA,NPA,FRA,FIA,AAA,YAINC,TTHA1,TTHA2,
     $WAVE,TLU,HF)
      WRITE(5,33)
370   LACW=0.0
      TW=0.0
35    WRITE(5,40)
      READ(5,41)(TLEW(K),K=1,32)
      WRITE(5,2)
      READ(5,1111)WWAVE
      DO36I=1,500
36    XINTW(I)=0.0
      PAUSE 'MOUNT THE DISC CONTAINING THE WORKED SAMPLE'
      READ(9'1)NPW
      DO25I=2,NPW+1
      READ(9'1)XINTW(I-1)
25    CONTINUE
37    WRITE(5,5)
      READ(5,1111)TTHW2
      WRITE(5,6)
      READ(5,1111)TTHW1
      YINCW=(TTHW2-TTHW1)/(NPW-1)
102   XMXW=0.0
      DO105I=1,NPW-2
      DINT=XINTW(I)+XINTW(I+1)+XINTW(I+2)
      IF(XMXW.GT.DINT)GOTO105
      XMXW=DINT
      IMXW=I+1
105   CONTINUE
      CALL BKGND(XINTW,NPW)
      CALL LRNTZ(WWAVE,TTHW1,NPW,XINTW,YINCW,TLU,TW,LACW,ALPHA)
      CALL FRCOF(IMXW,XINTW,NPW,FRW,FIW,AAA,YINCW,TTHW1,TTHW2,
     $WWAVE,TLU,HF)
      WRITE(6,47)PAGE,TLEW,DATEW,TIME
      WRITE(6,48)RADW,TTLOW,TW,MA,YINCW,LACW,KV,NPW,ALPHA,AAA,HF
      BAG=BRAGG*180./3.1416
60    WRITE(6,9)
      WRITE(6,10)
      SLPMX=0.
      DO170I=1,60
      IF(FRA(I).EQ.0..AND.FIA(I).EQ.0.)GOTO150
      FCCR(I)=(FRW(I)*FRA(I)+FIW(I)*FIA(I))/(FRA(I)**2+FIA(I)
     $**2)
      FCCI(I)=(FRW(I)*FIA(I)+FIW(I)*FRA(I))/(FRA(I)**2+FIA(I)
     $**2)
      GOTO155
150   FCCR(I)=0.
      FCCI(I)=0.
155   IF(I.LT.7)N=2*(I-1)
      IF(I.GT.6.AND.I.LT.12)N=5*(I-4)
      IF(I.GT.11)N=10*(I-8)
      ZZ=N/(AAA*HF)
      DIS=AAA*ZZ
      IF(I.EQ.1)GOTO170
      DDIS=DIS-DISO
      SLP=(FCCR(I-1)-FCCR(I))/DDIS
      IF(SLP.LT.SLPMX)GOTO170
      SLPMX=SLP
      AO=FCCR(I)+DIS*SLPMX
170   DISO=DIS
      DO6669I=1,60
      IF (FCCR(I).LE.0.) SAVE(I)=FCCR(I)
      IF (FCCR(I).LE.0.) FLAGS(I)='*'
```

```
      IF (FCCR(I).LE.0.) GO TO 6669
      SAVE(I)=ALOG(FCCR(I))
6669  CONTINUE
      DO175I=1,60
      FCCR(I)=FCCR(I)/A0
      FCCI(I)=FCCI(I)/A0
      LNFCR(I)=-11.51293
      IF(FCCR(I).GT.0.00001)LNFCR(I)=ALOG(FCCR(I))
172   IF(I.LT.7)N=2*(I-1)
      IF(I.GT.6.AND.I.LT.12)N=5*(I-4)
      IF(I.GT.11)N=10*(I-8)
      ZZ=N/(AAA*HF)
      DIS=AAA*ZZ
      WRITE(6,16)ZZ,FCCR(I),FCCI(I),LNFCR(I),DIS,FRW(I),
     #FIW(I),FRA(I),FIA(I),SAVE(I),FLAGS(I)
      IF(I/5*5.EQ.I)WRITE(6,18)
      IF((I-25)/45*45.NE.I-25)GOTO175
      PAGE=PAGE+1
      WRITE(6,47)PAGE,TLEW,DATEW,TIME
      WRITE(6,10)
175   CONTINUE
210   WRITE(5,31)
      READ(5,32)IANS
      IF(IANS.EQ.YES)GOTO370
      IF(IANS.NE.NO)GOTO210
215   WRITE(5,49)
      READ(5,32)IANS
      IF(IANS.EQ.YES)GOTO59
      IF(IANS.NE.NO)GOTO215
220   STOP
      END
      SUBROUTINEFRCOF(IMAX,XINT,NP,FR,FI,AAA,YINC,TTH1,
     #TTH2,WAVE,TLU,HF)
      WRITE(5,4444)
4444  FORMAT(/,' *FRCOF')
      REAL XSYM(251),XASYM(251),XINT(500),FR(60),FI(60)
1     FORMAT(' ',/,' YNORM=',F10.6)
5     FORMAT(' THE NUMBER OF POINTS IN RECIPROCAL SPACE',I5,
     #/,' HAS EXCEEDED THE PERMITTED VALUE OF 251. AN ERROR WILL
     #',/,' RESULT. CHANGE THE DIMENSIONS OF XSYM AND XASYM')
8     FORMAT(' THE MAXIMUM VALUE OF THE CALCULATED RECIPROCAL
     #SPACE COORDINATE',F8.3,/,' HAS EXCEEDED 0.5. THE FOURIER
     # COEF.S WHICH FOLLOW CONTAIN THIS ERROR.')
      RINC=YINC*3.1416/(2.0*180.)
      TMX=((TTH1+YINC*(IMAX-1))/2.)*3.1416/180.
      DELS=2.*AAA*(SIN(TMX+RINC)-SIN(TMX))/WAVE
      S1=2.*AAA*SIN(TMX)/WAVE
      S2=S1
      DO 9I=1,251
      XASYM(I)=0.0
9     XSYM(I)=0.0
      XSYM(1)=2.*XINT(IMAX)
      XASYM(1)=0.0
      MM=2.*AAA*(SIN(TMX)-SIN(TTH1*3.1416/(2.*180.)))/(DELS*WAVE)+1
      MMM=2.*AAA*(SIN(TTH2*3.1416/(2.*180.))-SIN(TMX))/(DELS*WAVE)+1
      IF(MMM.GT.MM)MM=MMM
      N=1
10    IF(MM.LE.251)GOTO15
      WRITE(5,5)MM
15    DO110I=1,MM-1
      FLG1=0.
      FLG2=0.
      S1=S1-DELS
      S2=S2+DELS
      T3=S1*WAVE/(2.*AAA)
      T5=SQRT(ABS(1-T3*T3))
```

```
      T1=ATAN(T3/T5)
      T4=(S2*WAVE/(2.*AAA))
      T6=SQRT(1-T4*T4)
      T2=ATAN(T4/T6)
      M=NP-IMAX
      IF(IMAX.GT.M)M=IMAX-1
      XHIGH=0.0
      XLOW=0.0
      DO100J=N,M+3
      TH1=TMX-J*RINC
      TH2=TMX+J*RINC
      IF(TH1.GT.T1.OR.FLG1.NE.0.)GOTO50
      JN=J
      FLG1=1.0
      IF(IMAX-J.GT.0)GOTO20
      XX1=0.0
      GOTO25
20    XX1=XINT(IMAX-J)
      IF(XX1.LT.0.)XX1=0.
25    IF(IMAX-J+1.GT.0)GOTO30
      XLOW=0.0
      GOTO50
30    XX2=XINT(IMAX-J+1)
      IF(XX2.LT.0.)XX2=0.
      XLOW=XX1+(XX2-XX1)*(T1-TH1)/RINC
50    IF(TH2.LT.T2.OR.FLG2.NE.0.0)GOTO90
      JM=J
      FLG2=1.0
      IF(IMAX+J.LT.NP+1)GOTO60
      YY1=0.0
      GOTO65
60    YY1=XINT(IMAX+J)
      IF(YY1.LT.0.)YY1=0.
65    IF(IMAX+J-1.LT.NP+1)GOTO70
      XHIGH=0.0
      GOTO90
70    YY2=XINT(IMAX+J-1)
      IF(YY2.LT.0.)YY2=0.
      XHIGH=YY1+(YY2-YY1)*(TH2-T2)/RINC
90    IF(FLG1.NE.1..OR.FLG2.NE.1.)GOTO100
      GOTO102
100   CONTINUE
102   XSYM(I+1)=XHIGH+XLOW
      XASYM(I+1)=XHIGH-XLOW
      P=I
      RAT=XSYM(I+1)/COS(3.14159265*DELS*P*HAR/(0.5))
      N=JN
      IF(JM.LT.JN)N=JM
      IF(I.EQ.1)GOTO110
      KI=I-1
110   CONTINUE
120   DO130I=1,60
      FR(I)=0.0
130   FI(I)=0.0
      Q=(KI-1)*DELS
      IF(Q.GT.0.5)WRITE(5,8)Q
      WRITE(5,5555)
5555  FORMAT(//,' A LENTHY CALCULATION HAS STARTED,
     #',/,' PROGRESS IS DOCUMENTED',//,' NOTE!
     #EXECUTION TERMINATES AT 0')
      ITEST=60
      DO150I=1,60
      WRITE(5,5556)ITEST
5556  FORMAT(' ',I2,$)
      IF(ITEST.EQ.30)WRITE(5,5557)
5557  FORMAT(' ')
```

```
      ITEST=ITEST-1
      IF(I.LT.7)N=2*(I-1)
      IF(I.GT.6.AND.I.LT.12)N=5*(I-4)
      IF(I.GT.11)N=10*(I-8)
      Z=N/(AAA*HF)
      DO145J=1,KI
      S=DELS*(J-1)
      B=.66666667
      IF(J/2*2.EQ.J)B=1.3333333
      IF(J.EQ.1)B=.33333333
      FR(I)=FR(I)+XSYM(J)*COS(3.1416*Z*S/0.5)*DELS*B
145   FI(I)=FI(I)+XASYM(J)*SIN(3.1416*Z*S/0.5)*DELS*B
      IF(I.EQ.1)YNORM=FR(1)
      FR(I)=FR(I)/YNORM
150   FI(I)=FI(I)/YNORM
      WRITE(5,1)YNORM
      RETURN
      END
      SUBROUTINEBKGND(XINT,NP)
      WRITE(5,1)
1     FORMAT(' *BKGND')
      REAL XINT(500)
      BKGMN=0.0
      BKGMX=0.0
      DO120I=1,9
      BKGMN=BKGMN+XINT(I)/9.0
120   BKGMX=BKGMX+XINT(NP+1-I)/9.0
      BGSLP=(BKGMX-BKGMN)/(NP-10)
      DO130I=1,NP
      XINT(I)=XINT(I)-(BKGMN+BGSLP*(I-5))
130   IF(I.LT.5.OR.I.GT.NP-5)XINT(I)=0.0
      RETURN
      END
      SUBROUTINELRNTZ(WAVE,TTH1,NP,XINT,YINC,TLU,T,LAC,ALPHA)
      WRITE(5,11)
11    FORMAT(/,' *LRNTZ')
      REAL LAC,XINT(500)
      INTEGER*4 YES,NO,IANS
      DATA YES/3HYES/
      DATA NO/3HNO /
1     FORMAT(' IS THE DATA FROM A THIN FILM?')
2     FORMAT(' ENTER THE LINEAR ABSORPTION COEF.',/,' L.A.C.=_')
3     FORMAT(' WHAT IS THE FILM THICKNESS IN CENTIMETERS'
     $,/,' T=_')
4     FORMAT(' WAS A MONOCHROMETER USED?')
5     FORMAT(' ENTER THE BRAGG ANGLE OF THE MONOCHROMETER.',/,
     $' ALPHA=_',$)
6     FORMAT(A3)
      IF(T.NE.0)GOTO30
10    WRITE(5,1)
      READ(5,6)IANS
      IF(IANS.EQ.NO)GOTO20
      IF(IANS.NE.YES)GOTO10
      WRITE(5,2)
      READ(5,1111)LAC
1111  FORMAT(F12.6)
      WRITE(5,3)
      READ(5,1111)T
      GOTO30
20    LAC=4
      T=4
30    ALPHA=0.0
      IANS=YES
35    WRITE(5,4)
      READ(5,6)IANS
      IF(IANS.EQ.NO)GOTO50
```

```
      IF(IANS.NE.YES)GOTO30
      WRITE(5,5)
      READ(5,1111)ALPHA
50    CSASQ=(COS(2*ALPHA*3.1416/180.0))**2
      DO40I=1,NP
      N=I-1
      TT=(TTH1+N*YINC)*3.1416/180.0
      XZ=-2.0*LAC*T/SIN(TT/2.0)
      T1=SIN(TT/2.)*SIN(TT/2.)
      TS=COS(TT)
      T3=TS*TS
      T2=COS(TT/2.)
      T4=EXP(XZ)
      XINT(I)=XINT(I)*SIN(TT)*(SIN(TT/2.0)/COS(TT/2.0))*((
     #1.0+COS(TT)**2.0)/(1.0+CSASQ*COS(TT)**2))/(1.0-EXP(-2.0
     #*LAC*T/SIN(TT/2)))
40    CONTINUE
      RETURN
      END
```

REFERENCES

1. Thompson, N., "Fracture," J. Wiley & Sons, New York (1959), pp. 354ff.

2. Forsyth, P. J. E. and C. A. Stubbington, J. Inst. Metals, Vol. 85, p. 339 (1956-57).

3. Cottrell, A. H. and D. Hull, Proc. Roy. Soc., Vol. 242, p. 211 (1957).

4. Alden, T. H. and A. Backofen, Acta Met., Vol. 9, p. 352 (1961).

5. Thompson, N. and N. J. Wadsworth, Adv. in Phys., Vol. 7, p. 72 (1958).

6. Grosskrentz, J. C., J. Appl. Phys., Vol. 34, p. 372 (1963).

7. McGrath, J. T. and W. J. Bratina, Phil. Mag., Vol. 11, p. 429 (1965).

8. Feltner, C. E. and C. Laird, Acta Met., Vol. 15, p. 1633 (1967).

9. Plumbridge, W. J. and D. A. Ryder, Met. Rev., Vol. 136, p. 119 (1969).

10. Segall, R. L., P. G. Partridge, and P. B. Hirsch, Phil. Mag., Vol. 6, p. 143 (1961).

11. McGrath, J. T. and G. W. J. Waldron, Phil. Mag., Vol. 9, p. 249 (1964).

12. Klesnil, M. and P. Lukas, J. Iron and Stell Inst., Vol. 203, p. 1043 (1965).

13. Laufer, E. E. and W. N. Roberts, Phil. Mag., Vol. 14, p. 65 (1966).

14. Levine, E. and S. Weissmann, Trans. Quar. Am. Soc. Metals, Vol. 61, p. 128 (1968).

15. Bennett, J. A., J. Research Natl. Bur. Standards, Vol. 46, p. 457 (1951).

16. Love, W. J., "Structural Changes in Ingot Iron Caused by Plastic and Repeated Stressing," Project HR-031-005, Rept T.A.M., Univ. of Illinois (Sep 1952).

17. Weissmann, S. and D. T. Evans, Acta Cryst., Vol. 7, p. 733 (1954).

18. Weissmann, S., J. Appl. Phys., Vol. 27, p. 389 (1956).

19. Pangborn, R. N., S. Weissmann, and I. R. Kramer, Scripta Met., Vol. 12, p. 129 (1978).

20. Pangborn, R. N., S. Weissmann, and I. R. Kramer, "Determination of Prefracture Fatigue Damage," Report No. DTNSRDC-80/006 (Jan 1980).

21. Pangborn, R. N., S. Weissmann, and I. R. Kramer, to be published in Met. Trans.

22. Stokes, A. R. and A. J. C. Wilson, Proc. Phys. Soc., London, Vol. 56 (1944), p. 174.

INITIAL DISTRIBUTION

Copies	
2	CNR 1 Code 465 1 Code 471
6	NRL 1 Code 6000 5 Code 6300
6	NAVSEA 1 SEA 035 1 SEA 05D 2 SEA 323 2 SEA 99612
2	NAVAIR AIR 320
12	DTIC
1	Air Force Materials Lab. Wright-Patterson AFB Dayton, OH 45433
1	Lehigh Univ. 327 Sinclair Lab Bldg 7 Bethlehem, PA 18015 (Dr. R. P. Wei)
1	Univ. of Maryland Dept. of Chemical Engrg. College Park, MD 20740 (R. Arsenault)
1	Massachusetts Institute of Technology Cambridge, MA 02130 (Dr. M. Cohen)
1	Northwestern Univ. Evanston, IL 60201 (Dr. J. Cohen)
10	Rutgers Univ. Piscataway, NJ 08854 (Dr. Weissmann)

Copies	
2	Syracuse Univ. Link Hall Syracuse, NY 13210 (Dr. Volkerweiss)
1	Ohio State Univ. Met. Eng. Dept. 116 W. 19th Ave. Columbus, OH 43210 (Dr. John R. Hirth)

CENTER DISTRIBUTION

Copies	Code	Name
2	012	R. Allen
1	012.1	D. Jewell
2	17	W. Murray
1	28	J. Belt
1	280	H. Singerman
15	2802	I. Kramer
2	281	G. Wacker
6	282	J. Crisci
10	5211.1	Repts Distribution
1	522.1	Library (C)
1	522.2	Library (A)
2	5231	Office Services

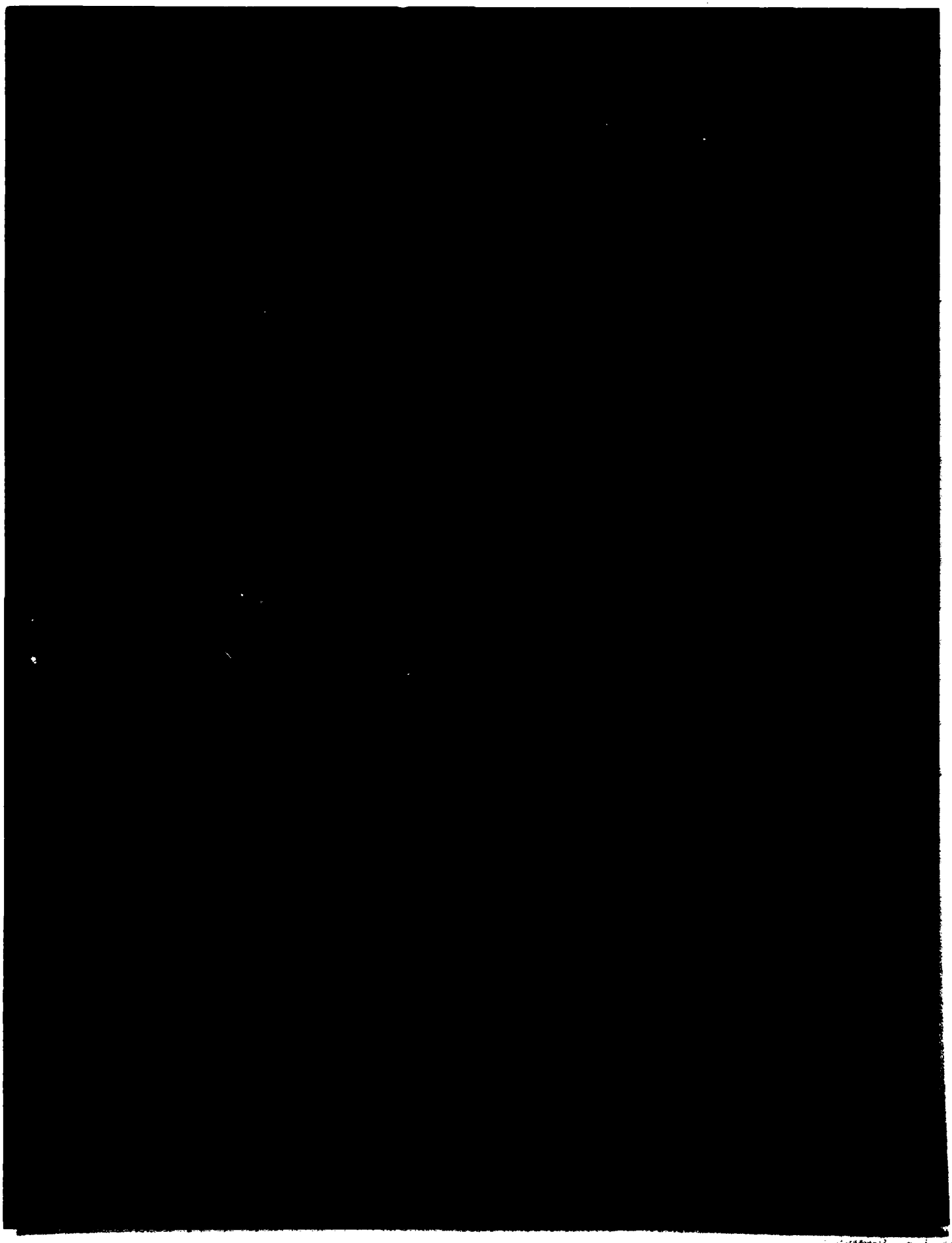


DAT
FILM